

2012

MUC1 mucin stabilizes and activates hypoxia-inducible factor 1 alpha to regulate metabolism in pancreatic cancer

Nina V. Chaika

University of Nebraska Medical Center, nchaika@unmc.edu

Teklab Gebregiworgis

University of Nebraska-Lincoln, tgebregiworgis2@unl.edu

Michelle E. Lewallen

University of Nebraska Medical Center

Vinee Purohit

University of Nebraska Medical Center

Prakash Radhakrishnan

University of Nebraska Medical Center, pradhakr@unmc.edu

See next page for additional authors

Follow this and additional works at: <http://digitalcommons.unl.edu/chemistrypowers>

Chaika, Nina V.; Gebregiworgis, Teklab; Lewallen, Michelle E.; Purohit, Vinee; Radhakrishnan, Prakash; Liu, Xiang; Zhang, Bo; Mehla, Kamiya; Brown, Roger B.; Caffrey, Thomas; Yu, Fang; Johnson, Keith R.; Powers, Robert; Hollingsworth, Michael A.; and Singh, Pankaj K., "MUC1 mucin stabilizes and activates hypoxia-inducible factor 1 alpha to regulate metabolism in pancreatic cancer" (2012). *Robert Powers Publications*. 57.

<http://digitalcommons.unl.edu/chemistrypowers/57>

This Article is brought to you for free and open access by the Published Research - Department of Chemistry at DigitalCommons@University of Nebraska - Lincoln. It has been accepted for inclusion in Robert Powers Publications by an authorized administrator of DigitalCommons@University of Nebraska - Lincoln.

Authors

Nina V. Chaika, Teklab Gebregiworgis, Michelle E. Lewallen, Vinee Purohit, Prakash Radhakrishnan, Xiang Liu, Bo Zhang, Kamiya Mehla, Roger B. Brown, Thomas Caffrey, Fang Yu, Keith R. Johnson, Robert Powers, Michael A. Hollingsworth, and Pankaj K. Singh

MUC1 mucin stabilizes and activates hypoxia-inducible factor 1 alpha to regulate metabolism in pancreatic cancer

Nina V. Chaika^a, Teklab Gebregiworgis^{b,1}, Michelle E. Lewallen^{a,1}, Vinee Purohit^{a,c,1}, Prakash Radhakrishnan^{a,1}, Xiang Liu^a, Bo Zhang^b, Kamiya Mehla^a, Roger B. Brown^a, Thomas Caffrey^a, Fang Yu^d, Keith R. Johnson^{a,e,f,g}, Robert Powers^b, Michael A. Hollingsworth^{a,c,e}, and Pankaj K. Singh^{a,e,f,2}

^aEppley Institute for Research in Cancer and Allied Diseases, University of Nebraska Medical Center, Omaha, NE 68198; ^bDepartment of Chemistry, University of Nebraska–Lincoln, Lincoln, NE 68588; Departments of ^cPathology and Microbiology, ^dBioinformatics, ^eBiochemistry and Molecular Biology, and ^fGenetic Cell Biology and Anatomy, University of Nebraska Medical Center, Omaha, NE 68198; and ^gDepartment of Oral Biology, College of Dentistry, University of Nebraska Medical Center, Omaha, NE 68198

Edited by Gregg L. Semenza, The Johns Hopkins University School of Medicine, Baltimore, MD, and approved July 11, 2012 (received for review February 28, 2012)

Aberrant glucose metabolism is one of the hallmarks of cancer that facilitates cancer cell survival and proliferation. Here, we demonstrate that MUC1, a large, type I transmembrane protein that is overexpressed in several carcinomas including pancreatic adenocarcinoma, modulates cancer cell metabolism to facilitate growth properties of cancer cells. MUC1 occupies the promoter elements of multiple genes directly involved in glucose metabolism and regulates their expression. Furthermore, MUC1 expression enhances glycolytic activity in pancreatic cancer cells. We also demonstrate that MUC1 expression enhances in vivo glucose uptake and expression of genes involved in glucose uptake and metabolism in orthotopic implantation models of pancreatic cancer. The MUC1 cytoplasmic tail is known to activate multiple signaling pathways through its interactions with several transcription factors/coregulators at the promoter elements of various genes. Our results indicate that MUC1 acts as a modulator of the hypoxic response in pancreatic cancer cells by regulating the expression/stability and activity of hypoxia-inducible factor-1 α (HIF-1 α). MUC1 physically interacts with HIF-1 α and p300 and stabilizes the former at the protein level. By using a ChIP assay, we demonstrate that MUC1 facilitates recruitment of HIF-1 α and p300 on glycolytic gene promoters in a hypoxia-dependent manner. Also, by metabolomic studies, we demonstrate that MUC1 regulates multiple metabolite intermediates in the glucose and amino acid metabolic pathways. Thus, our studies indicate that MUC1 acts as a master regulator of the metabolic program and facilitates metabolic alterations in the hypoxic environments that help tumor cells survive and proliferate under such conditions.

cancer metabolism | glutamine accumulation | pentose phosphate pathway | 2-ketoglutarate

MUC1, a type I transmembrane protein, plays a significant role in the progression of cancer, particularly pancreatic adenocarcinoma (1–4). Although expressed in the normal pancreas, its expression is elevated in pancreatic adenocarcinoma and its expression pattern changes from a strictly apical localization on normal polarized epithelial cells to a broad distribution across the cell surface membrane of nonpolarized tumor cells (2). This results in aberrant signaling that enhances tumor progression and metastasis. MUC1 protein is expressed in >90% of pancreatic tumors (5), and MUC1 expression in tumors and its serum levels are associated with a poor prognosis and recurrence in patients with resected tumors (6). Much of the oncogenic role of MUC1 can be attributed to the participation of the small, cytoplasmic tail of MUC1 (MUC1.CT) in signal transduction and transcriptional events (2). ChIP-chip analyses have demonstrated that MUC1 occupies a plethora of promoter elements in which MUC1 modulates the recruitment and activity of

transcription factors, thus regulating transcription of the corresponding genes (7).

Several studies have established a role for MUC1 in tumor growth, invasion and metastasis in pancreatic cancer (4, 8, 9). MUC1 expression significantly correlates with tumor cell growth and invasiveness in vitro and tumor growth and metastasis in the orthotopic injection models of pancreatic cancer (3, 4). MUC1-overexpressing cells (S2-013.MUC1) produced larger tumors than the mock-transfected S2-013 cells (S2-013.Neo), indicating that MUC1 overexpression facilitates tumor growth (3). Pancreatic cancer cells metastasize to liver, lung, lymph nodes, and other tissues in patients with pancreatic cancer. MUC1 overexpression in pancreatic cancer cells significantly enhances the number of metastases in lymph nodes and lungs in orthotopic implantation models (3). Furthermore, mice lacking MUC1 have a profound defect in tumor growth and metastasis (1). These mice also have defects in MAPK activity and oncogenic signaling.

Pancreatic tumors exhibit significant levels of desmoplasia that results in hypoxic microenvironments (10, 11). Hypoxia is known to stabilize the activity of hypoxia-inducible factors (HIFs) that reprogram cancer cell metabolism to facilitate cancer cell growth in harsh environments (12–14). HIFs can also be stabilized by several oncogenes, which act through hypoxia-independent mechanisms. HIF-1 α activates transcription of several genes regulating glucose uptake, glycolysis, and flux through the tricarboxylic acid cycle. Thus, increased protein levels of HIF-1 α result in increased glucose metabolism through the glycolytic pathway, but reduced entry of glucose into the TCA cycle (12). Such metabolic alterations provide the tumor cells with increased biomass production, thus enhancing proliferation.

Here, we present data implicating MUC1 as a facilitator of glucose uptake and glycolysis in pancreatic cancer cells. In addition, we demonstrate that MUC1 physically occupies promoter regions and regulates expression of multiple metabolic genes. Furthermore, we show that MUC1 enhances HIF-1 α stabilization and activity in pancreatic cancer cells. Our metabolomic

Author contributions: N.V.C., T.G., M.E.L., K.R.J., R.P., M.A.H., and P.K.S. designed research; N.V.C., T.G., M.E.L., V.P., P.R., X.L., B.Z., K.M., R.B.B., and T.C. performed research; M.E.L., F.Y., and P.K.S. contributed new reagents/analytic tools; N.V.C., T.G., M.E.L., V.P., P.R., B.Z., F.Y., R.P., and P.K.S. analyzed data; and K.R.J., R.P., M.A.H., and P.K.S. wrote the paper.

The authors declare no conflict of interest.

This article is a PNAS Direct Submission.

¹T.G., M.E.L., V.P., and P.R. contributed equally to this work.

²To whom correspondence should be addressed. E-mail: pankaj.singh@unmc.edu.

This article contains supporting information online at www.pnas.org/lookup/suppl/doi:10.1073/pnas.1203339109/-DCSupplemental.

analysis demonstrates that MUC1 acts as a master regulator of the metabolic program in pancreatic cancer.

Results

MUC1 Physically Occupies Promoters of Key Metabolic Enzymes and Regulates Their Activity. Activation of MUC1. CT signaling in response to various growth factors leads to differential gene expression (2). To further investigate the mechanism by which MUC1. CT activation triggers differential gene expression, we performed ChIP-chip promoter analysis. We used CT2 mAb, which recognizes MUC1. CT, to pull down the sonicated DNA elements that were occupied by MUC1 in S2-013.MUC1F cells, and the DNA elements were then identified by performing a promoter microarray analysis, as described previously (7). Results from these studies showed that the promoters of several metabolic genes are physically occupied by MUC1 (Fig. S1 A and C). We confirmed *ENO1* and *PGM2* promoter occupancy by MUC1 in independent ChIP studies (Fig. S1 B and D).

MUC1 Regulates Expression of Glycolytic Genes. To determine if MUC1 regulates the expression of glycolytic genes, we performed real-time quantitative PCR (qPCR) analysis of RNA extracted from control (S2-013.Neo), MUC1-overexpressing (S2-013.MUC1), vector control [FG.shScr (scrambled control)], and MUC1-knockdown (FG.shMUC1) cells cultured under normoxic or hypoxic conditions (at 1% oxygen), which enhance glycolytic gene expression (15). The relative mRNA expression levels for HK2, PFKFB2, *ENO1*, *PGK1*, *PGM2*, and *LDHA* are shown in Fig. S2A. These results indicate that MUC1 has an additive role with hypoxia on some of the glycolytic gene promoters (e.g., *LDHA*), whereas, on others (e.g., *PGK1*, *PGM2*), there is synergism between MUC1 and hypoxia.

MUC1 Regulates Glucose Uptake and Lactate Production in Pancreatic Cancer Cells. As MUC1 occupies promoters of multiple genes involved in glycolysis, we then determined the effect of MUC1 expression on glucose uptake and lactate production. To achieve this, we performed glucose uptake assays in S2-013.MUC1 or S2-013.Neo cells by using [³H]2-deoxyglucose (DG). Cells treated with labeled and excess unlabeled 2-DG were used as controls to set a baseline for nonspecific tritium uptake. After normalization for total cell count, we observed a twofold increase in glucose uptake by S2-013.MUC1 in comparison with S2-013.Neo cells (Fig. S2B). Similarly, we observed a more than twofold reduction in glucose uptake upon knockdown of MUC1 expression in FG.shMUC1 cells in comparison with FG.shScr (Fig. S2C). These results demonstrate that MUC1 expression facilitates glucose uptake in pancreatic adenocarcinoma cells. Levels of lactate, an end product of aerobic glycolysis, were also similarly modulated by MUC1 (Fig. S2 B and C).

MUC1 Regulates in Vivo Glucose Uptake in an HIF-1 α -Dependent Manner. Next, we sought to determine if the differences in the rate of glucose uptake were not simply an artifact of cell culture. To achieve this, we implanted the S2-013.MUC1 or S2-013.Neo cells orthotopically into the pancreas of athymic female nude mice. Three weeks later, the mice were injected with IR800 dye-coupled 2-DG (IRDye 800CW 2DG; LI-COR Biosciences). The mice were imaged 24 h after injection. We observed significantly higher glucose uptake by tumors generated from S2-013.MUC1 cells than the tumors generated from S2-013.Neo cells (Fig. 1A). The glucose uptake values were quantified by normalizing to the tumor size (Fig. S3) determined by euthanizing the animals after glucose measurements (Fig. 1B). Similar results were obtained with orthotopically implanted Capan1.MUC1 and Capan1.neo cells (Fig. 1B). However, MUC1-mediated increase in glucose uptake was significantly diminished by HIF-1 α knockdown (Fig.

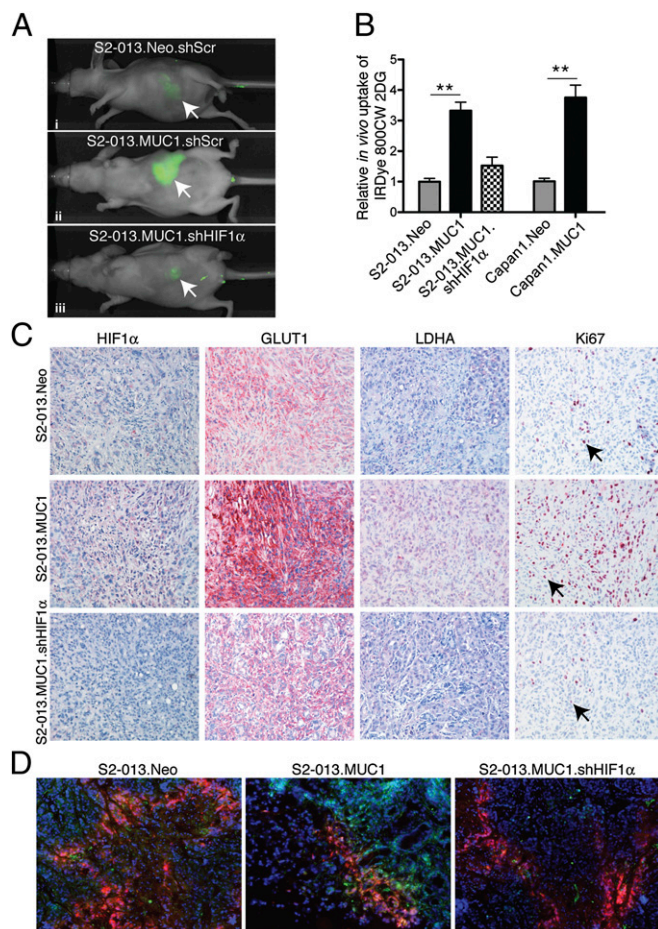


Fig. 1. MUC1 regulates in vivo glucose uptake and expression of glycolytic genes. (A) Glucose uptake by tumors formed by orthotopically implanted S2-013.Neo.shScr (scrambled control), S2-013.MUC1.shScr (scrambled control), or S2-013.MUC1.shHIF-1 α (HIF-1 α knockdown). Orthotopic xenograft tumors in athymic nudes were imaged with IRDye 800CW 2DG. Arrowheads indicate the tumors. (B) Quantification of in vivo glucose uptake by tumors (normalized to tumor size). (C) Immunohistochemical staining of formalin-fixed paraffin-embedded tumor sections reveals increased expression of HIF-1 α , GLUT1, and LDHA and increased nuclear Ki67 staining in S2-013.MUC1 cells in comparison with S2-013.Neo cells. Arrowheads point to nuclear Ki67 staining. (D) Immunofluorescence staining for hypoxia (EF5, red), HIF-1 α (green), and nuclei (DAPI) in tumor sections from S2-013.Neo, S2-013.MUC1, and S2-013.MUC1.shHIF-1 α -implanted mice (* P < 0.05 and ** P < 0.01).

1B). Also, we determined the expression of genes involved in aerobic glycolysis in the tumor sections from orthotopic implantation models with S2-013.Neo and S2-013.MUC1 cells (Fig. 1C). The expression of HIF-1 α , GLUT1, and LDHA was significantly more enhanced in tumors from S2-013.MUC1 cells in comparison with that of S2-013.Neo cells. Also, S2-013.MUC1 cells exhibited higher staining levels of Ki67, a marker of cell proliferation, compared with the S2-013.Neo cells (Fig. 1C). The increases in the expression of glycolytic genes were abrogated by HIF-1 α knockdown (Fig. 1C). Reciprocally, MUC1 knockdown in orthotopically implanted cells expressing naturally high levels of MUC1 (Capan2.shMUC1 vs. Capan2.shScr) demonstrated decreased glucose uptake (Fig. S4). Immunofluorescent EF5 staining indicated that, although the hypoxia levels were similar in the different tumor groups, MUC1 expressing tumor sections demonstrated enhanced HIF-1 α levels (Fig. 1D). These results

confirm that MUC1 overexpression enhances glucose uptake in pancreatic cancer cells.

MUC1 Regulates Expression/Stability and Activity of HIFs. As our data indicated an additive effect of hypoxia on MUC1-mediated transcriptional activation of glycolytic genes, we next examined if MUC1 modulated the stability of hypoxia-inducible transcription factors at protein level. By performing Western blot analysis, we evaluated if culturing S2-013.MUC1 cells under hypoxia-mimicking conditions (CoCl₂, which stabilizes HIFs) differentially altered the expression of HIF-1 α and HIF-2 α in comparison with the control S2-013.Neo. Our CoCl₂ dose-course (Fig. S5A) and time-course (Fig. S5B) experiments suggest that MUC1 expression enhances expression/stabilization of HIF-1 α and HIF-2 α in pancreatic cancer cells. However, the increased expression of HIF-1 α under conditions of MUC1 overexpression is not caused by changes in mRNA levels of HIF-1 α or the prolyl hydroxylase domain-containing proteins (PHDs)/von Hippel–Lindau tumor suppressor protein (VHL) that regulate HIF-1 α turnover (Fig. S6). S2-013.MUC1 cells also demonstrated increased expression of HK2, GLUT1, and PDK1 at protein level, in contrast to the S2-013.Neo cells (Fig. S5C). We performed lentiviral shRNA-mediated knockdown of HIF-1 α in S2-013.Neo and S2-013.MUC1 cells. HIF-1 α knockdown, but not scrambled control, diminished hypoxia mimetic-induced expression of the glycolytic gene HK2 (Fig. S5D). Furthermore, by performing promoter-reporter assays by using hypoxia response element (HRE)-containing human *enolase (ENO) 1* promoter-Luciferase reporter constructs, we observed that S2-013.MUC1 cells exhibited higher HRE-promoter activity under treatment with DMOG, which inhibits PHDs and stabilizes HIF-1 α (Fig. S5E) (16). Strikingly, even when transfected with constitutively active HIF-1 α , which has been rendered resistant to proteasomal degradation via deletion of part of the oxygen-dependent domain of HIF-1 α and mutation of specific prolyl residues (17), S2-013.MUC1 cells exhibited higher activity than S2-013.Neo cells (Fig. S5E). Thus, we can infer that MUC1 enhances HIF-1 α activity, independent of its effect on HIF-1 α expression levels. MUC1 expression also enhanced hypoxia-induced glucose uptake in S2-013 and Capan1 pancreatic cancer cell lines (Fig. S5F–G). Knockdown of HIF-1 α in S2-013.MUC1 cells reverted MUC1 overexpression-induced increase in glucose uptake (Fig. S5F). Reciprocally, the expression levels of MUC1 were also induced by hypoxic conditions in

a HIF-1 α -dependent manner (Fig. S5H and I). Furthermore, knockdown of MUC1 in Capan2 pancreatic cancer cell line diminished hypoxia-induced increase in the expression levels of HIF-1 α , HK2, and GLUT1 (Fig. S7A and B). Also, MUC1 knockdown in Capan2 diminished glucose uptake and lactate production (Fig. S7C and D). As MUC1 and HIF-1 α facilitate expression of some of the same glycolytic genes, we tested if the synergist activity is a result of their physical interaction. Proximity ligation assays (PLAs) demonstrate significant MUC1 and HIF-1 α interaction in S2-013.MUC1 and FG cells under HIF-1 α stabilizing conditions (Fig. 2A and B). Also, we could coimmunoprecipitate HIF-1 α with MUC1 by using an mAb against MUC1.CT, from S2-013.MUC1 cells treated with CoCl₂ or solvent control (Fig. 2C).

MUC1 Facilitates Hypoxia-Dependent Recruitment of HIF-1 α and p300 to Glycolytic Gene Promoters. Next, we sought to ask if MUC1 expression enhances occupancy of glycolytic gene promoters by HIF-1 α . To achieve this, S2-013.Neo and S2-013.MUC1 cells were cultured under normoxic or hypoxic conditions (1% oxygen) for 4 h and subjected to ChIP assays with HIF-1 α Ab. qPCR assays with the immunoprecipitated chromatin indicated increased HIF-1 α occupancy on *ENO1* and *PGM2* glycolytic gene promoter regions containing functional HREs; $-109/+44$ (i.e., flanking sequence and 44 nt inside the transcription start site) for *ENO1* and $-63/+52$ for *PGM2* (Fig. 3A) (16). No enrichment was observed for the distal regions. Furthermore, MUC1 coimmunoprecipitated with p300, a HIF-1 α coactivator, in a hypoxia-dependent manner (Fig. 3B). ChIP assays revealed p300 occupancy at *ENO1* and *PGM2* HRE regions, which was significantly enhanced by hypoxic conditions. The p300 occupancy was further enhanced by MUC1 overexpression in a hypoxia-dependent manner (Fig. 3C). The levels of histone H3 acetylated at lysine-9 (H3K9-ac) at *ENO1* and *PGM2* HREs was also significantly enhanced by MUC1 overexpression in a hypoxia-dependent manner (Fig. 3D). MUC1 overexpression had no effect on total cellular levels of H3K9-Ac or histone 3 (Fig. 3E).

MUC1 as Global Metabolic Regulator. To identify the effect of MUC1 on global metabolite levels in pancreatic adenocarcinoma cells, we performed NMR-based differential metabolomic studies. Principle component analysis of one-dimensional ¹H NMR spectra obtained from unlabeled S2-013.Neo and S2-013.MUC1

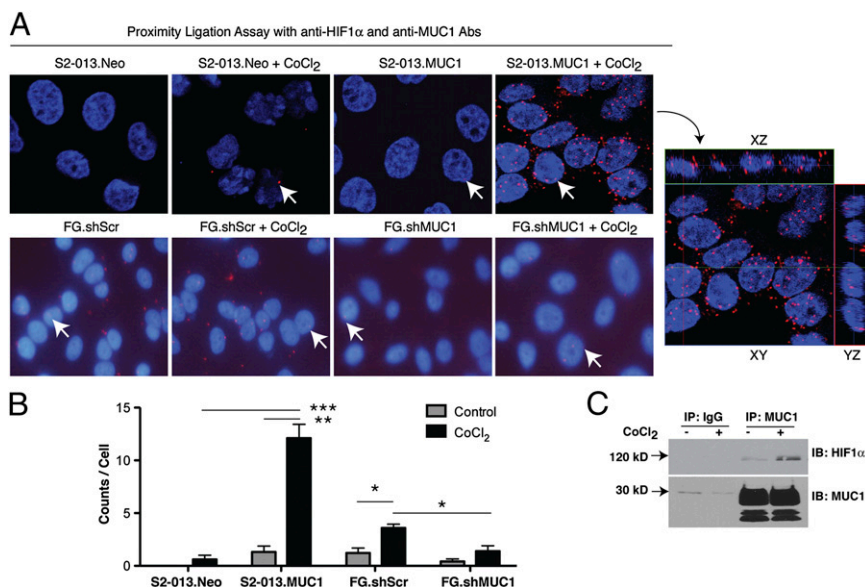
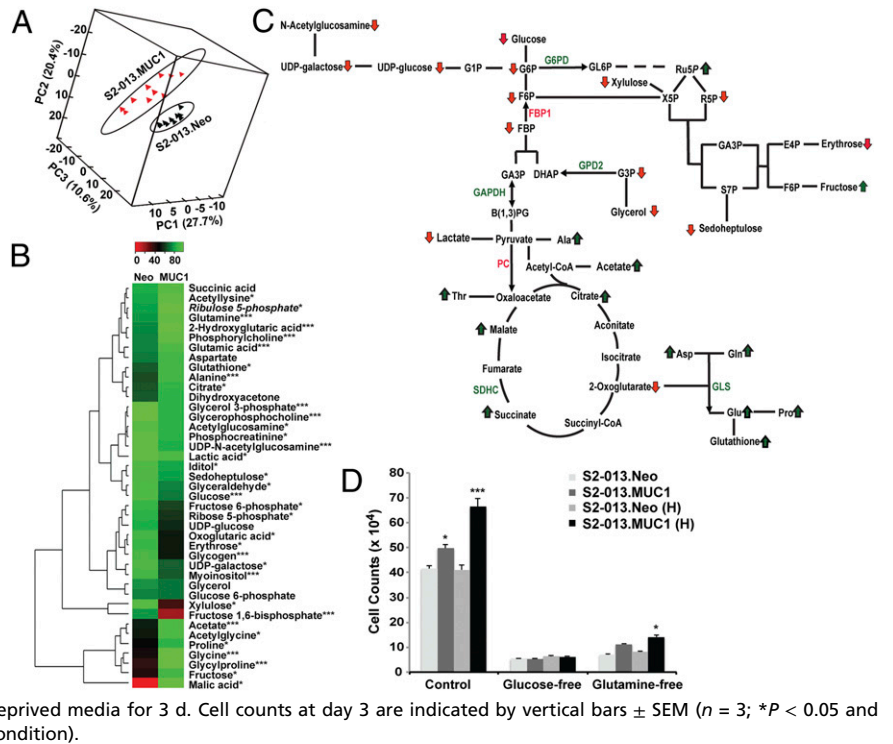


Fig. 2. Interaction of MUC1.CT with HIF-1 α . (A) PLA with Abs against MUC1.CT (CT2) and HIF-1 α demonstrate increased interaction of MUC1 with HIF-1 α under conditions of MUC1 expression and 6 h CoCl₂ treatment. Arrowheads point to the interaction spots. *Right*: 3D localization of interaction spots in S2-013.MUC1 cells under CoCl₂ treatment. (B) Quantification of interaction spots per cell in S2-013.Neo, S2-013.MUC1, FG.shScr, and FG.shMUC1 cells under conditions of 6 h CoCl₂ treatment or control. (C) Coimmunoprecipitation of HIF-1 α along with MUC1 from Nonidet P-40 extracts of 6 h CoCl₂ treated or control S2-013.MUC1 cells. Immunoprecipitations with isotype IgG were performed as a control (* $P < 0.05$, ** $P < 0.01$, and *** $P < 0.001$).

Fig. 4. MUC1 regulates metabolite levels in pancreatic cancer cells. (A) Three-dimensional principal component analysis scores plot comparing S2-013.Neo cells (black) with S2-013.MUC1 cells (red). (B) Heat map generated from the normalized-mean peak intensities for each metabolite identified from the triplicate set of 2D ^1H - ^{13}C HSQC NMR experiments. The normalized-mean intensities are plotted on a color-scale from 0% (red) to 100% (green). Dendrogram depicts hierarchical clustering of relative metabolite concentration changes between the S2-013.MUC1 and S2-013.Neo cells ($*P < 0.05$ and $***P < 0.001$; metabolites in italics have lower levels of confidence in NMR peak assignment). (C) Metabolic pathway depicting the metabolites identified in the S2-013.MUC1 and S2-013.Neo cell cultures by the 2D ^1H - ^{13}C HSQC NMR experiments. Three replicates of S2-013.MUC1 and S2-013.Neo cell cultures were used for metabolite identification. Dark green arrows correspond to metabolites with an increased concentration in S2-013.MUC1 cells relative to S2-013.Neo cells. Arrows colored red correspond to metabolites with a decreased concentration in S2-013.MUC1 cells relative to S2-013.Neo cells. Metabolic genes up- or down-regulated by MUC1 expression are indicated by green and red, respectively. Most glycolytic genes are not depicted for clarity. (D) Cells (5×10^4) were seeded and cultured under normoxic or hypoxic conditions (1% O_2) in regular or glucose/glutamine-deprived media for 3 d. Cell counts at day 3 are indicated by vertical bars \pm SEM ($n = 3$; $*P < 0.05$ and $***P < 0.001$ vs. counts of S2-013.Neo cells for that condition).



previous studies that suggest a role of MUC1 in modulating growth and invasive properties in multiple cancer types (3, 4). Increased tumor cell metabolism has been identified as a hallmark of cancer and a requirement for rapid tumor cell growth.

Our data demonstrate that MUC1 interacts with HIF-1 α and regulates the stability/activity of the latter. HIF-1 α stability is regulated by prolyl hydroxylation. Under well-oxygenated conditions, HIF-1 α is hydroxylated on Pro-402 and/or Pro-564 by PHD2, which uses oxygen and 2-oxoglutarate, also known as α -ketoglutarate, as substrates in a reaction that generates CO_2 and succinate as byproducts (12). Prolyl hydroxylation of HIF-1 α triggers its interaction with the von Hippel-Lindau tumor suppressor protein, which recruits an E3-ubiquitin ligase that targets HIF-1 α for proteasomal degradation. Under hypoxic conditions, the prolyl hydroxylation is inhibited by substrate (i.e., O_2) deprivation and/or the mitochondrial generation of reactive oxygen species, which may oxidize Fe(II) present in the catalytic center of the hydroxylases (12). Furthermore, metabolic alterations that result in depletion of oxoglutarate facilitate stabilization of HIF-1 α . Our metabolomic data indicates that MUC1 expression decreases the intracellular levels of 2-oxoglutarate, which may be the reason for increased stabilization of HIF-1 α under conditions of MUC1 expression. Treatment of S2-013.Neo or S2-013.MUC1 cells with excess 2-oxoglutarate diminishes MUC1-dependent increase in the levels of HIF-1 α (Fig. S8).

Previous studies have demonstrated that MUC1 itself is a target of HIF-1 α (18). Thus, increased stabilization of HIF-1 α might be a part of a positive feedback loop that may serve to promote tumorigenesis and metastasis in cancer cells. Our studies are in contrast to the previous studies by Yin et al. in HCT116 and ZR-75-1 cells, in which the authors demonstrate PHD3 down-regulation-mediated decreased stabilization of HIF-1 α by MUC1 (19). Interestingly, even Yin et al. identified that MUC1 causes a decrease in the expression of PHD2 (19), the major prolyl hydroxylase for HIF-1 α in most cell types. However, the decreased stabilization of HIF-1 α by MUC1 in their studies could reflect cell type-specific dependence of HIF-

1 α on PHD3. Regardless of which PHD is the major regulator of HIF-1 α stabilization, 2-oxoglutarate is a critical substrate for the reaction. Hence, our metabolomic studies indicating a decrease in the levels of 2-oxoglutarate by MUC1 clearly suggest that MUC1 causes a decrease in PHD activity that results in HIF-1 α stabilization in pancreatic cancer cells. Our mRNA expression data indicating an increase in the levels of PHD1-2 as a result of MUC1 suggests that the cells try to recover from the decreased PHD activity by increasing the mRNA levels (Fig. S6). A similar phenomenon is observed under hypoxic conditions in which PHD activity is significantly depleted as a result of a lack of oxygen substrate.

Furthermore, MUC1 physically occupies the promoter regions of and selectively enhances the transcription of some of the glycolytic genes in a HIF-dependent manner. Our studies indicate that MUC1 co-occupies promoter elements of glycolytic genes along with HIF-1 α . Also, MUC1 modulates glycolytic promoter occupancy by HIF-1 α and p300 and thus H3K9 acetylation status and HIF-1 α transcriptional activity in pancreatic cancer. There are at least two potential mechanisms whereby MUC1 could modulate the effects of hypoxia signaling through the HIF transcription factors: by regulating HIF stability and interaction partners and thereby directly modifying HIF signaling; and by direct signaling through the MUC1.CT, in a manner in which MUC1 directly associates with transcription factors (e.g., p53, β -catenin, and ER α) (2). Our studies demonstrate that MUC1 regulates HIF stability, HIF activity, p300 recruitment, and histone acetylation status on HIF-inducible promoters and that MUC1 can induce the expression of hypoxia-inducible genes in an HIF-dependent manner. The MUC1-dependent increase in p300 recruitment and H3K9 acetylation at HRE elements of glycolytic gene promoters may explain MUC1-mediated increase in HRE-luciferase activity under expression of constitutively stabilized HIF-1 α .

Our NMR-based metabolomics studies indicate that MUC1 facilitates glucose and amino acid metabolism in pancreatic cancer cells. We observed decreased accumulation of glucose, glycolytic intermediates, and lactate in S2-013.MUC1 cells, in contrast to S2-013.Neo cells. Metabolomic studies indicate the

kinetics of metabolic reactions in the cells. Hence, the decreased accumulation of glucose, glycolytic intermediates, and lactate, despite higher glucose uptake rate and increased secretion of lactate in the culture media, indicates that S2-013.MUC1 cells have faster glucose turnover, in contrast to S2-013.Neo cells. It is evident that glucose and amino acid metabolic pathways are critical for the production of biosynthetic intermediates, and thus for rapid tumor cell growth (20). We observed increased flux through glycolysis and pentose phosphate pathways. Increased levels of ribose 5-phosphate may account for increased nucleotide biosynthesis in S2-013.MUC1 cells in comparison with the S2-013.Neo cells. Also, we observed increased levels of amino acids, including glutamine, which may explain MUC1-dependent increase in cell growth even under conditions of glutamine deprivation. In fact, our analysis of Ki67 levels in tumor sections suggest that MUC1-facilitated HIF-1 α stability/activity promotes cancer cell growth under hypoxic conditions in the pancreatic tumor model. These findings are critical because HIF-1 α is a key modulator of glycolysis in cancer and HIF-1 α has been implicated in tumorigenesis. Furthermore, compared with the normal tissues, which are well oxygenated, metastasizing tumor cells intermittently switch between hypoxic and aerobic conditions. This leads to stabilization and activation of HIF-1 α , which in turn facilitates aerobic glycolysis in tumors.

In summary, we have presented findings that MUC1 serves as a metabolic regulator that facilitates the transcription of multiple genes involved in the glucose metabolic pathways. Also, we present a mechanistic relationship between MUC1 and HIF-1 α , whereby MUC1 may increase the stability of HIF-1 α by diminishing the levels of 2-oxoglutarate. We also present evidence that MUC1 physically interacts with HIF-1 α and p300 in a hypoxia-dependent manner, and enhances promoter occupancy of the HIF-1 α and p300 on glycolytic gene promoters. The interrelationship between MUC1–HIF-1 α oncogenic signaling networks serves to facilitate tumor growth and metastasis and could present a potential therapeutic target for the treatment of malignant diseases that rely upon MUC1 and HIF-1 α .

Materials and Methods

Cells and Reagents. Cell culture media and conditions are described in *SI Materials and Methods*. DMOG (Cayman Chemical) was dissolved in DMSO, and CoCl₂ (Sigma) was dissolved in DMEM.

ChIP and qPCR Assays. ChIP assays and qPCR assays were performed as described in *SI Materials and Methods*. The qPCR primer sequences are given in Table S1. For ChIP qPCR analysis, values were normalized to a genomic region located within the β -glucuronidase (*GUSB*) gene and expressed as fold increase vs. enrichment detected by using IgG as published previously (7). The average expression \pm SEM was reported.

Immunoblotting, Immunoprecipitation, and PLAs. Western blotting and immunoprecipitations were performed as previously described (21, 22). The membranes were probed with primary antibodies against HIF-1 α (Santa Cruz Biotechnology), MUC1 (Abcam), GLUT1 (Abcam), HK2 (Cell Signaling Technology), and LDHA (Abcam). In situ PLA experiments were performed as described in *SI Materials and Methods*.

Animal Studies, Immunohistochemistry, and Hypoxia Imaging. Animal studies, immunohistochemistry and hypoxia imaging were performed as described in *SI Materials and Methods*.

Metabolomic Analysis. S2-013.Neo or S2-013.MUC1 cells (1.5×10^7) were used for NMR-based metabolomic analysis. The details of metabolite extraction and one-dimensional ¹H NMR spectra and 2D ¹H-¹³C HSQC spectra analysis are described in *SI Materials and Methods*. The peaks were assigned to individual metabolites by using the chemical shift references from the Human Metabolomics Database (23). KEGG (24) database was used for drawing the metabolite network.

Statistical Analysis. Nonparametric Kruskal–Wallis tests were used to compare differences between cell lines. If the overall Kruskal–Wallis test indicated a difference in cell lines, a Wilcoxon rank-sum test was performed for each pairwise comparison of interest. Student *t* test was used when appropriate. *P* < 0.05 was considered significant.

ACKNOWLEDGMENTS. This work was supported in part by Specialized Programs for Research Excellence [SPORE; National Cancer Institute (NCI)] in Gastrointestinal/Pancreatic Cancer Grant P50 CA127297 (to M.A.H. and K.R.J.), NCI SPORE Career Development Award P50 CA127297 (to P.K.S.), NCI SPORE Developmental Research Project Award P50 CA127297 (to P.K.S.), NCI R01 CA163649 to P.K.S., NCI R01 CA057362 to M.A.H., National Institute of General Medical Sciences (NIGMS) Centers of Biomedical Research Excellence (CoBRE) P20 GM103489 to K.R.J., NCI Early Diagnosis of Pancreatic Cancer Grant U01 CA111294 (to M.A.H.), NCI Grant R21 CA137401 (to K.R.J.), National Institutes of Health National Center for Research Resources Grant P20 RR-17675 (to R.P.), NCI Pancreatic Tumor Microenvironment Research Network Grant U54 CA163120 (to K.R.J., M.A.H., and P.K.S.), and Gretchen Swanson Center for Nutrition (GSCN) Cancer Prevention and Control nutrition Seed Grant 15618 (to P.K.S.).

- Besmer DM, et al. (2011) Pancreatic ductal adenocarcinoma mice lacking mucin 1 have a profound defect in tumor growth and metastasis. *Cancer Res* 71:4432–4442.
- Singh PK, Hollingsworth MA (2006) Cell surface-associated mucins in signal transduction. *Trends Cell Biol* 16:467–476.
- Singh PK, et al. (2007) Platelet-derived growth factor receptor beta-mediated phosphorylation of MUC1 enhances invasiveness in pancreatic adenocarcinoma cells. *Cancer Res* 67:5201–5210.
- Tsutsumida H, et al. (2006) RNA interference suppression of MUC1 reduces the growth rate and metastatic phenotype of human pancreatic cancer cells. *Clin Cancer Res* 12: 2976–2987.
- Qu CF, et al. (2004) MUC1 expression in primary and metastatic pancreatic cancer cells for in vitro treatment by (213)Bi-C595 radioimmunoconjugate. *Br J Cancer* 91: 2086–2093.
- Ho JJ, Chung YS, Yuan M, Henslee JG, Kim YS (1992) Differences in expression of SPan-1 and CA15-3 antigens in blood and tissues. *Int J Cancer* 52:693–700.
- Behrens ME, et al. (2010) The reactive tumor microenvironment: MUC1 signaling directly reprograms transcription of CTGF. *Oncogene* 29:5667–5677.
- Kohlgraf KG, et al. (2003) Contribution of the MUC1 tandem repeat and cytoplasmic tail to invasive and metastatic properties of a pancreatic cancer cell line. *Cancer Res* 63:5011–5020.
- Satoh S, et al. (2000) Enhancement of metastatic properties of pancreatic cancer cells by MUC1 gene encoding an anti-adhesion molecule. *Int J Cancer* 88:507–518.
- Hidalgo M, Maitra A (2009) The hedgehog pathway and pancreatic cancer. *N Engl J Med* 361:2094–2096.
- Neesse A, et al. (2011) Stromal biology and therapy in pancreatic cancer. *Gut* 60: 861–868.
- Semenza GL (2010) HIF-1: Upstream and downstream of cancer metabolism. *Curr Opin Genet Dev* 20:51–56.
- Bertout JA, Patel SA, Simon MC (2008) The impact of O₂ availability on human cancer. *Nat Rev Cancer* 8:967–975.
- Rundqvist H, Johnson RS (2010) Hypoxia and metastasis in breast cancer. *Curr Top Microbiol Immunol* 345:121–139.
- Brahimi-Horn MC, Chiche J, Pouyssegur J (2007) Hypoxia signalling controls metabolic demand. *Curr Opin Cell Biol* 19:223–229.
- Semenza GL, et al. (1996) Hypoxia response elements in the aldolase A, enolase 1, and lactate dehydrogenase A gene promoters contain essential binding sites for hypoxia-inducible factor 1. *J Biol Chem* 271:32529–32537.
- Kelly BD, et al. (2003) Cell type-specific regulation of angiogenic growth factor gene expression and induction of angiogenesis in nonischemic tissue by a constitutively active form of hypoxia-inducible factor 1. *Circ Res* 93:1074–1081.
- Aubert S, et al. (2009) MUC1, a new hypoxia inducible factor target gene, is an actor in clear renal cell carcinoma tumor progression. *Cancer Res* 69:5707–5715.
- Yin L, Kharbanda S, Kufe D (2007) Mucin 1 oncoprotein blocks hypoxia-inducible factor 1 α activation in a survival response to hypoxia. *J Biol Chem* 282:257–266.
- DeBerardinis RJ, Lum JJ, Hatzivassiliou G, Thompson CB (2008) The biology of cancer: metabolic reprogramming fuels cell growth and proliferation. *Cell Metab* 7:11–20.
- Wen Y, Caffrey TC, Wheelock MJ, Johnson KR, Hollingsworth MA (2003) Nuclear association of the cytoplasmic tail of MUC1 and beta-catenin. *J Biol Chem* 278: 38029–38039.
- Singh PK, et al. (2008) Phosphorylation of MUC1 by Met modulates interaction with p53 and MMP1 expression. *J Biol Chem* 283:26985–26995.
- Wishart DS, et al. (2009) HMDB: A knowledgebase for the human metabolome. *Nucleic Acids Res* 37(Database issue):D603–D610.
- Kanehisa M, et al. (2008) KEGG for linking genomes to life and the environment. *Nucleic Acids Res* 36(database issue):D480–D484.

Supporting Information

Chaika et al. 10.1073/pnas.1203339109

SI Materials and Methods

Cells and Reagents. Capan1 and Capan2 cells were obtained from American Type Culture Collection. S2-013 is a cloned subline of a human pancreatic tumor cell line (SUIT-2) derived from a liver metastasis (1). The S2-013 cells were cultured as previously described (2). FG cell line is a liver metastatic derivative of colo357 cells (3). shRNA-mediated knockdowns of MUC1 and hypoxia-inducible factor (HIF)-1 α were established by using the target sequences described elsewhere (4, 5). MUC1-overexpressing variants of S2-013 and Capan1 cells have been described previously (6, 7).

Glucose Uptake Assay. Cells (5×10^4) were seeded per well in a 24-well plate. Twelve hours later, the cells were starved for glucose for 2 h and then incubated for 20 min with 1 μ Ci [3 H]2-deoxyglucose (DG) for a glucose uptake assay. Cells were lysed with 1% SDS and the lysates were counted for [3 H] by using a scintillation counter. Cells treated with labeled and excess unlabeled 2-DG were used as controls to set a baseline for nonspecific tritium uptake. The results were normalized to the cell counts for treated and untreated groups. Data are presented as the mean value of triplicate values of glucose uptake normalized with control cells.

Lactate Assay. Lactate levels secreted in the media were analyzed by colorimetric assays. The assay was performed as per the manufacturer's protocol by using a Lactate Assay Kit II (BioVision).

Luciferase Assays. Hypoxia response element (HRE) luciferase plasmid was obtained from Addgene (8). PGL2 basic was used as a control plasmid for transfection in luciferase studies. A dual luciferase reporter assay (Promega) was used to detect promoter activity in this study. A synthetic *Renilla* luciferase reporter plasmid pRL-SV40 (Promega) was used as a control for transfection efficiency. The assays were performed as described previously (7). Each experiment was performed three times in triplicate.

ChIP and Real-Time PCR Assays. ChIP assays were performed as described previously (6). cDNA was generated by using SuperScript III First-strand Synthesis Kit (Invitrogen). Reactions containing 2.0 μ L cDNA for gene expression analysis or 3.0 μ L purified chromatin for ChIP analysis were prepared in SYBR Green master mix (Applied Biosystems) and subjected to quantitative real-time PCR analysis by using an ABI 7500 thermocycler. Each reaction was repeated in triplicate, and the experiments were repeated at least twice to confirm reproducibility. Values were obtained for the threshold cycle (Ct) for each gene or genomic region, and data were analyzed using the standard curve method. For real-time PCR analysis, values were normalized to the expression of β -actin, and average expression \pm SEM was reported. Primer sequences are given in Table S1. For ChIP PCR analysis, values were normalized to a genomic region located within the β -glucuronidase (*GUSB*) gene and expressed as a fold increase vs. enrichment detected by using IgG, as published previously (6). The average expression \pm SEM was reported.

Proximity Ligation Assay. In situ proximity ligation assay (PLA) experiments were performed by using DuoLink II (Olink Bioscience). Cells were incubated overnight at 4 $^{\circ}$ C with anti-MUC1

(Abcam) diluted 1:500 and/or anti-HIF-1 α (Santa Cruz Biotechnology) diluted 1:50 in blocking buffer. Samples were then washed with PBS solution and incubated with PLA probes DII anti-mouse/hamster MINUS, DII anti-mouse/hamster PLUS, DII anti-rabbit MINUS, or DII anti-rabbit PLUS in combinations suitable for single or dual recognition. Control experiments were included by omitting the primary antibody used for single recognition PLA or either one of the primary antibodies used in double recognition PLA. The subsequent washing steps, ligation, rolling-circle amplification and fluorescent labeling with DuoLink II Detection Reagent Orange were performed according to the manufacturer's instructions (Olink Bioscience). Slides with PLA samples were mounted in DuoLink II Mounting Media with DAPI (Olink Bioscience). A Zeiss LSM 510 microscope equipped with a Zeiss image processing system was used for confocal imaging. A 63 \times /1.4 oil objective and sequential scanning with filters appropriate to each fluorophore was used (420–480 nm for DAPI, 505–530 nm for EGFP, 560–615 nm for CY3, and long-pass 560 nm for PLA signals). Images used for PLA quantification were captured and processed with identical settings. PLA signals of individual cells were counted in five individual confocal images and a minimum of 50 cells per sample.

Tumor Growth and in Vivo Glucose Uptake Studies. Congenitally athymic female nude mice (NCR-nu/nu) were purchased from the National Cancer Institute. Mice were treated in accordance with institutional animal care and use committee guidelines. Cells (5×10^5) were used for orthotopic injections into the pancreas of nude mice, as described previously (9). A total of 12 to 14 mice were used for each cell type/condition. When the tumors were palpable, the mice were injected i.p. with 100 μ L of 10 nM IR800 dye-coupled 2-DG (IRDye 800CW 2DG; LI-COR Biosciences) with or without glucose (2 g/kg body weight; control). The mice were imaged 24 h after injection by using Pearl Impulse, a near-IR in vivo imager (LI-COR Biosciences).

Immunohistochemistry and Hypoxia Imaging. Immunohistochemistry was performed by using goat anti-rabbit IgG-AP with Fast-Red to produce red stain (Picture-Double Staining kit; Invitrogen) per manufacturer instructions. The following primary antibodies were used: GLUT1 (Abcam), HIF-1 α (Santa Cruz Biotechnology), Ki67 (Thermo Fisher), and LDHA (Abcam). The stained sections were imaged at 20 \times under an inverted microscope. Cells with Ki67-positive nuclear staining were counted in five random fields at 20 \times magnification. To image for hypoxia, tumor-bearing animals were injected with EF5 at 3 h before euthanasia (10). After the animals were euthanized, tumor sizes were measured with calipers. Flash-frozen tumor sections were then stained with cy3-conjugated anti-EF5 serum, Alexa-488 anti-HIF-1 α , and DAPI. Stained sections were imaged for immunofluorescence.

Extraction of Metabolites. S2-013.Neo or S2-013.MUC1 cells (15×10^6) were harvested from the culture plate by trypsinization. The harvested cells were then osmotically lysed in sterile water and sonicated. The cell lysates were stored in a freezer at -80° C until extraction. Frozen cell lysates were lyophilized to dryness and suspended in 1 mL methanol. The suspension was vortexed to mix the cell lysates with the methanol thoroughly. The samples were then centrifuged at 18000 \times g for 1 min to spin down the cell debris. The supernatant was lyophilized by using a freeze dryer (Labconco). The dried samples were dissolved by using 600 μ L deuterated 50 mM potassium phosphate buffer, pH 7.2 (un-

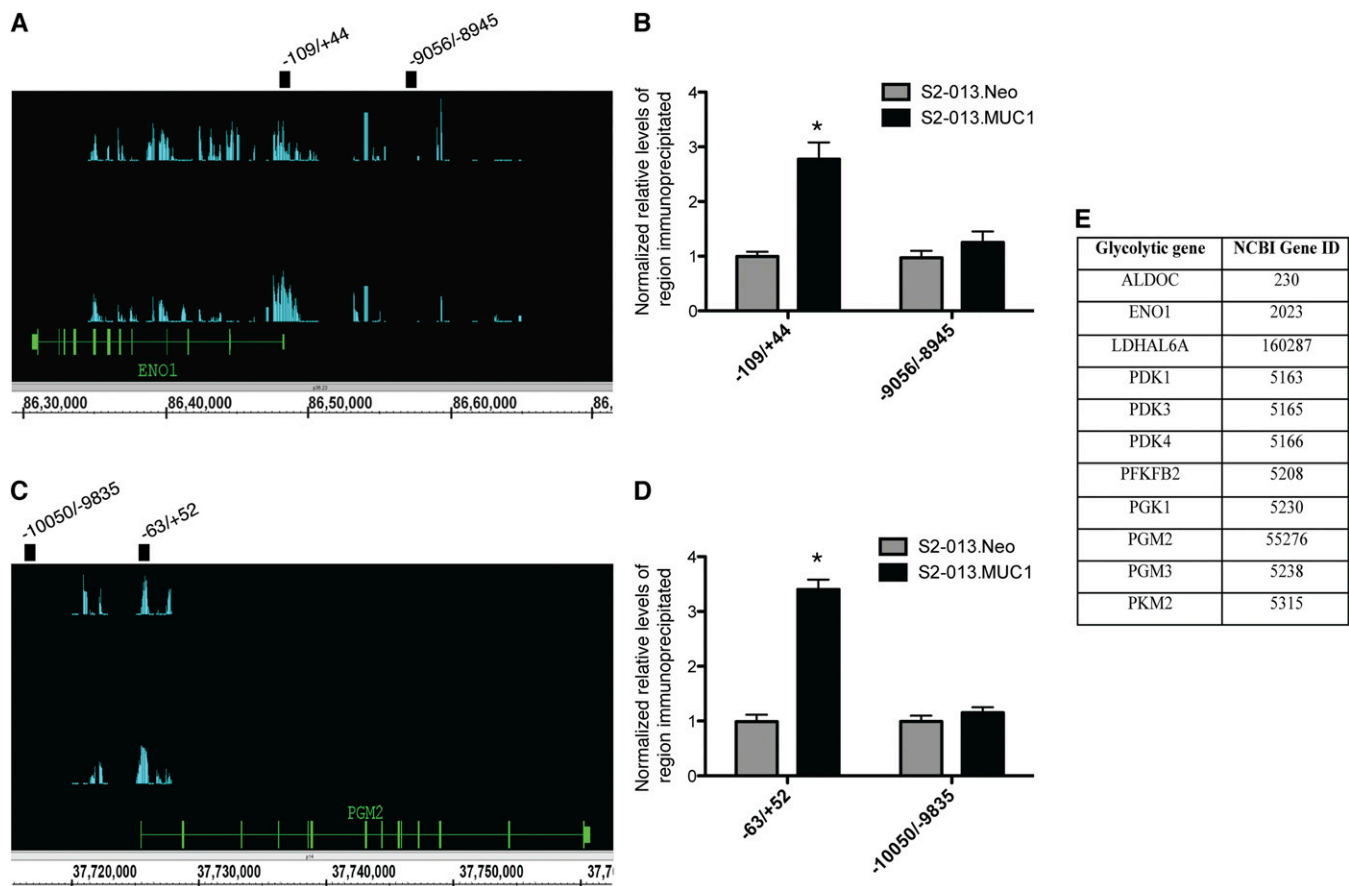


Fig. S1. Occupancy of glycolytic gene promoters by MUC1.CT. (A) ChIP-chip analysis revealed MUC1.CT occupies regions within the *ENO1* gene, the proximal promoter, and upstream regions of the *ENO1* promoter. Image from Integrated Genome Browser (Affymetrix) shows two experimental ChIP-chip replicates in which vertical lines represent individual oligonucleotide probes whose height represents degree of enrichment. Oligonucleotide primer pairs used to confirm MUC1.CT occupancy are represented by black bars. (B) Occupancy of *ENO1* promoter by MUC1.CT was confirmed by ChIP using anti-MUC1.CT antibody (CT2) or IgG control, followed by quantitative PCR (qPCR) analysis. Enrichment of proximal and distal *ENO1* promoter regions was detected in S2-013.MUC1 cells, whereas no enrichment was observed in S2-013.Neo cells ($*P < 0.05$). (C) ChIP-chip analysis revealed promoter occupancy of *PGM2* promoter by MUC1.CT in two independent experiments. (D) Occupancy of *PGM2* promoter by MUC1.CT was confirmed by ChIP using anti-MUC1.CT antibody (CT2) or IgG control, followed by qPCR analysis in S2-013.Neo and S2-013.MUC1 cells ($*P < 0.05$ vs. S2-013.Neo). (E) List of metabolic genes whose promoters are occupied by MUC1.CT, as determined by ChIP-chip analysis.

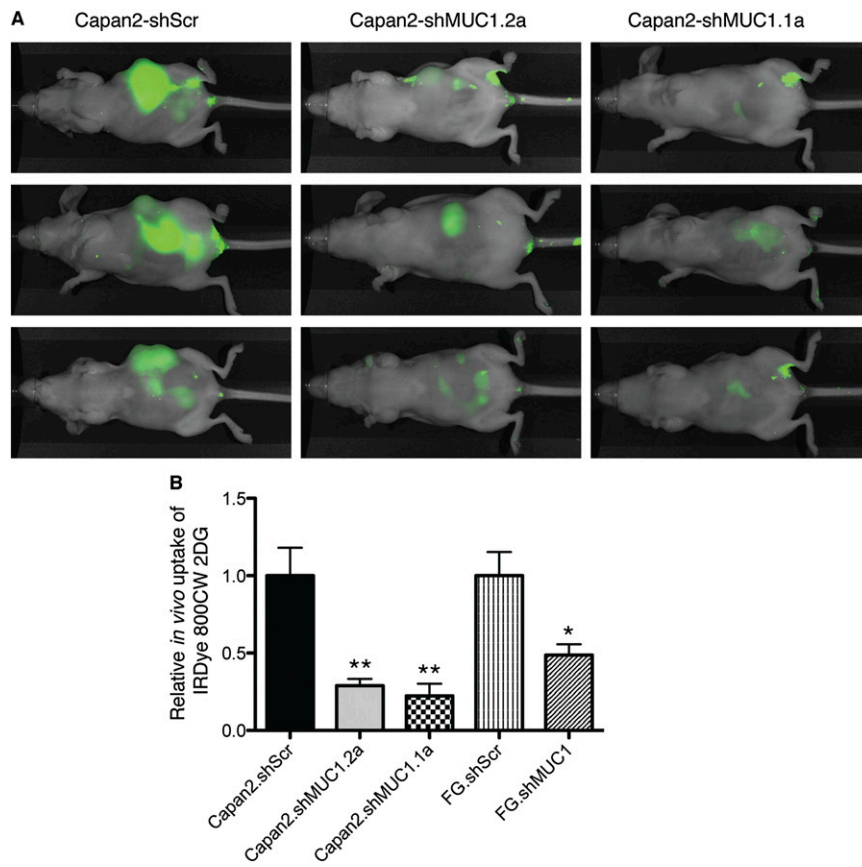


Fig. S4. Effect of MUC1 knockdown on in vivo glucose uptake. (A) Glucose uptake by tumors formed by orthotopically implanted Capan2.shScr (scrambled control), Capan2.shMUC1.2a (MUC1 knockdown target 2), or Capan2.shMUC1.1a (MUC1 knockdown target 1). (B) Quantitation of in vivo glucose uptake by tumors formed by orthotopically implanted Capan2.shScr, Capan2.shMUC1.2a or Capan2.shMUC1.1a, FG.shScr, or FG.shMUC1 cells. * $P < 0.05$, ** $P < 0.01$.

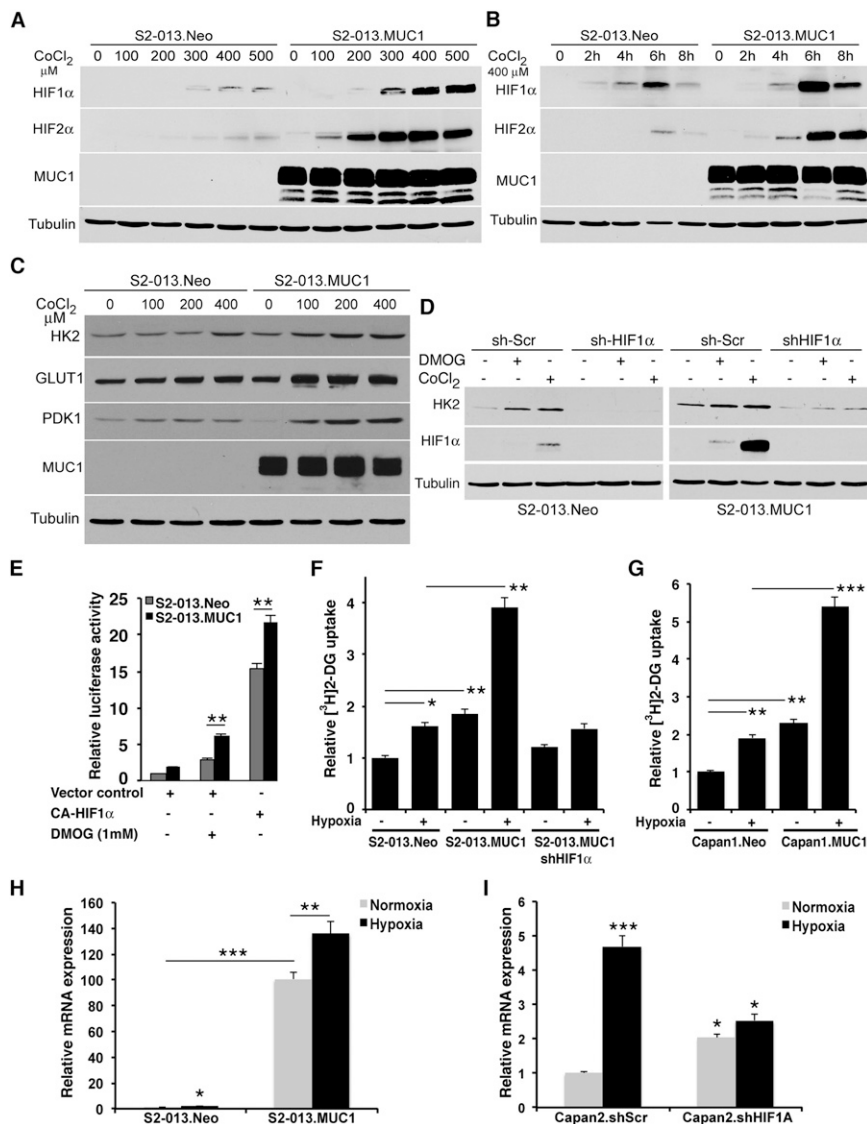


Fig. S5. Effect of MUC1 on HIF expression and activity. (A) Immunoblotting to demonstrate the effect of different doses of 6 h of hypoxia-mimetic CoCl₂ treatment on the expression of HIF-1α and HIF-2α at protein levels in S2-013.Neo and S2-013.MUC1 cells. (B) Effect of different durations of 400 μM dose of CoCl₂ treatment on the expression of HIF-1α and HIF-2α in S2-013.Neo and S2-013.MUC1 cells by immunoblotting. (C) Immunoblotting to demonstrate effect of MUC1 on expression of HK2, GLUT1, and PDK1 in S2-013.Neo and S2-013.MUC1 cells under treatment with different doses of hypoxia mimetic CoCl₂ for 12 h. (D) HIF-1α knockdown abrogates MUC1-induced up-regulation of glycolytic enzyme HK2. The cells were infected with lentiviral particles carrying HIF-1α targeting sequences or scrambled control (Scr). Knockdown of HIF-1α and its effect on HK2 expression was determined by Western blotting. (E) Effect of MUC1 on HIF-1α activity was determined by *ENO1*-HRE promoter-luciferase reporter assays. S2-013.Neo or S2-013.MUC1 cells were transiently transfected for 36 h with *ENO1*-HRE-luc, Renilla-luc, constitutively active HIF-1α (CA-HIF-1α), or vector control, and then treated with 1 mM DMOG or PBS solution control for 8 h, and the luciferase counts were obtained on a luminometer by using a Stop-N-Glow Dual Reporter System. The fold change values presented here have been normalized with Renilla-Luc activity. (F and G) Effect of MUC1 and HIF-1α on glucose uptake under hypoxia (1% oxygen) was determined by using [³H]2DG in S2-013.Neo, S2-013.MUC1, S2-013.MUC1.shHIF1α, Capan1.Neo, or Capan1.MUC1 cells. (H and I) Effect of hypoxia-mediated activation of HIF-1α and HIF-1α knockdown on MUC1 mRNA levels. S2-013.Neo, S2-013.MUC1 and S2-013.MUC1.shHIF1α, Capan2.shScr, or Capan2.shHIF1A cells were cultured under normoxia or 48 h hypoxia, and the mRNA levels of MUC1 were detected by qPCR (**P* < 0.05, ***P* < 0.01, and ****P* < 0.001).

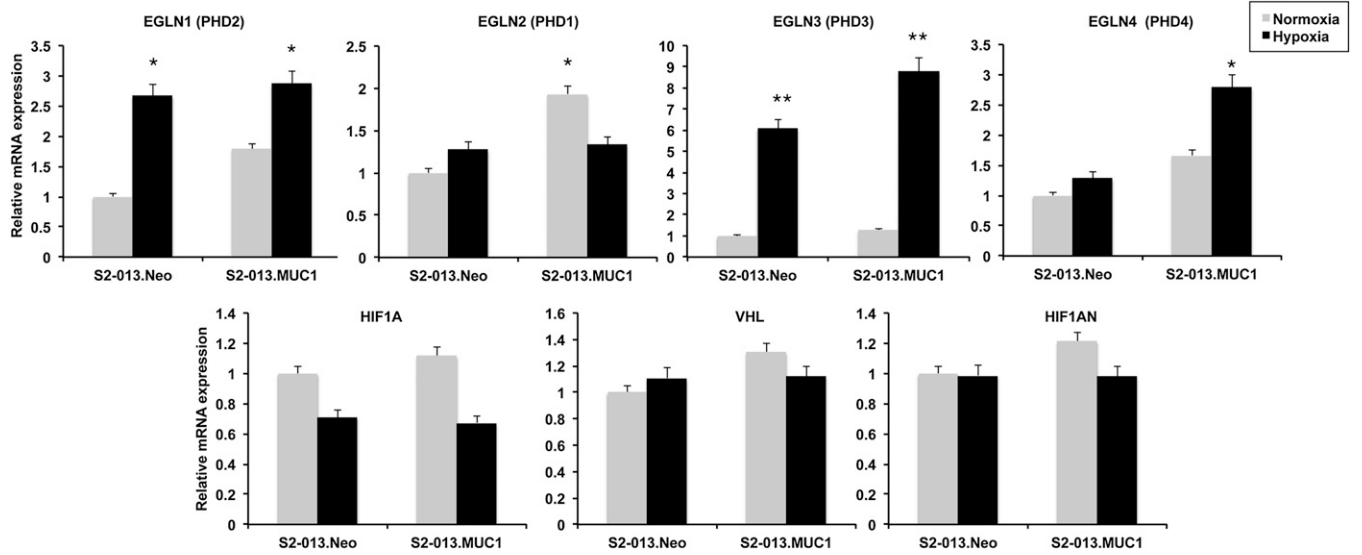


Fig. 56. Effect of MUC1 overexpression on the mRNA levels of PHDs, HIF-1 α , von Hippel-Lindau tumor suppressor protein (VHL), and HIF-1AN. qPCR reveals MUC1 and hypoxia-dependent changes in the mRNA levels of PHDs. qPCR analysis reveals no significant change in the expression of HIF-1 α , von Hippel-Lindau tumor suppressor protein, and HIF-1AN at mRNA level by MUC1, comparing S2-013.MUC1 with S2-013.Neo. * $P < 0.05$, ** $P < 0.01$.

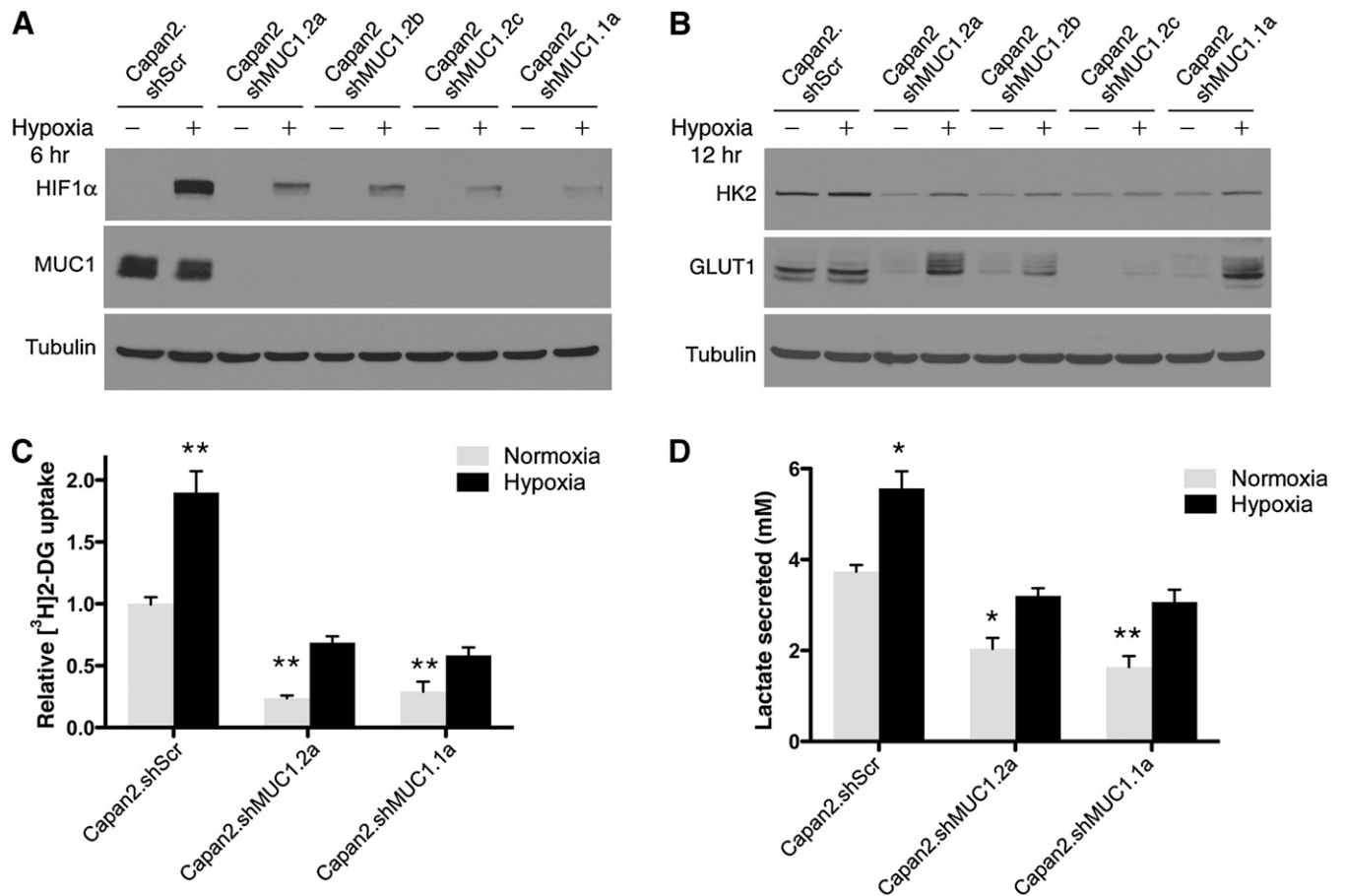


Fig. 57. Effect of MUC1 knockdown on HIF-1 α expression and activity. (A) Immunoblotting to demonstrate the effect of 6 h of hypoxia treatment on the expression of HIF-1 α at protein levels in Capan2.shScr and multiple clones of MUC1-knockdown Capan2 (2a, 2b, 2c, and 1a) cells. (B) Immunoblotting to demonstrate the effect of 12 h of hypoxia treatment on the expression of HK2 and GLUT1 in MUC1 knockdown or control Capan2 cells. (C) Relative glucose uptake in MUC1-knockdown Capan2 clones relative to Capan2.shScr as determined by [3 H]2-DG uptake assays. (D) Amount of lactate secreted by scrambled control and MUC1-knockdown Capan2 cells as measured by colorimetric assays. * $P < 0.05$, ** $P < 0.01$.

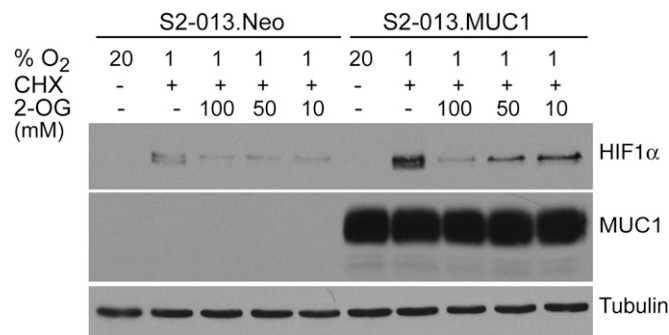


Fig. S8. 2-Oxoglutarate (2-OG) abrogates MUC1-induced increase in the protein levels of HIF-1 α . S2-013.Neo and S2-013.MUC1 cells were incubated under normoxic or hypoxic conditions (1% O₂). After 2 h hypoxia incubation, the cells were subjected to treatment with 20 μ M cycloheximide (CHX) and different doses of 2-oxoglutarate and then incubated under hypoxia for another 2 h. The levels of HIF-1 α , MUC1, and tubulin were determined by immunoblotting.

Table S1. Primer sequences for real-time PCR

Primer	Sequence
HK2-F	GAGCCACCACTCACCTACT
HK2-R	ACCCAAGCACACGGAAGTT
PFKFB2-F	ATGACCAACTCCCCGACTCT
PFKFB2-R	TGGACACGTAGGTTTTACCCC
ENO1-F	CTGGTGCCGTTGAGAAGGG
ENO1-R	GGTTGTGGTAAACCTCTGCTC
PGK1-F	TTAAAGGGAAGCGGGTCGTTA
PGK1-R	TCCATTGTCCAAGCAGAATTTGA
PGM2-F	GAGGCAGTGAACGACTAATAGC
PGM2-R	GAAATTCAGGTCCCATAGCAG
LDHA-F	CTCCAAGCTGGTCATTATCACG
LDHA-R	AGTTCGGGCTGTATTTTACAACA
HIF1A-F	CGTTCCTTCGATCAGTTGTC
HIF1A-R	TCAGTGGTGGCAGTGGTAGT
ACTB-F	GTCCACCGCAAATGCTTCTA
ACTB-R	TGCTGTACACCTTCACCGTTC
HIF1AN-F	TTCCCGACTAGGCCCATTC
HIF1AN-R	CAGGGCAGGATACACAAGATT
EGLN1-F	GAAGGCGAACCTGTACCCC
EGLN1-R	CATGCACGGCACGATGTACT
EGLN2-F	AGGCCCCAAACGGAAATG
EGLN2-R	AGGGCACGATATAGTCCAGGG
EGLN3-F	TCTCCCGAGAGTTGCGAGAAA
EGLN3-R	AGAGGGAACGATCTACACGAG
EGLN4-F	ACGCCGCGATCAAGGCTGAC
EGLN4-R	GCAGCACCCCTCTGGCGGATG
VHL-F	GACCTGGAGCGGCTGACA
VHL-R	TACCATCAAAGCTGAGATGAAACA
MUC1-F	CTGCTCCTCACAGTGCTTACAGTTG
MUC1-R	TGAACCGGGGCTGTGGCTGG